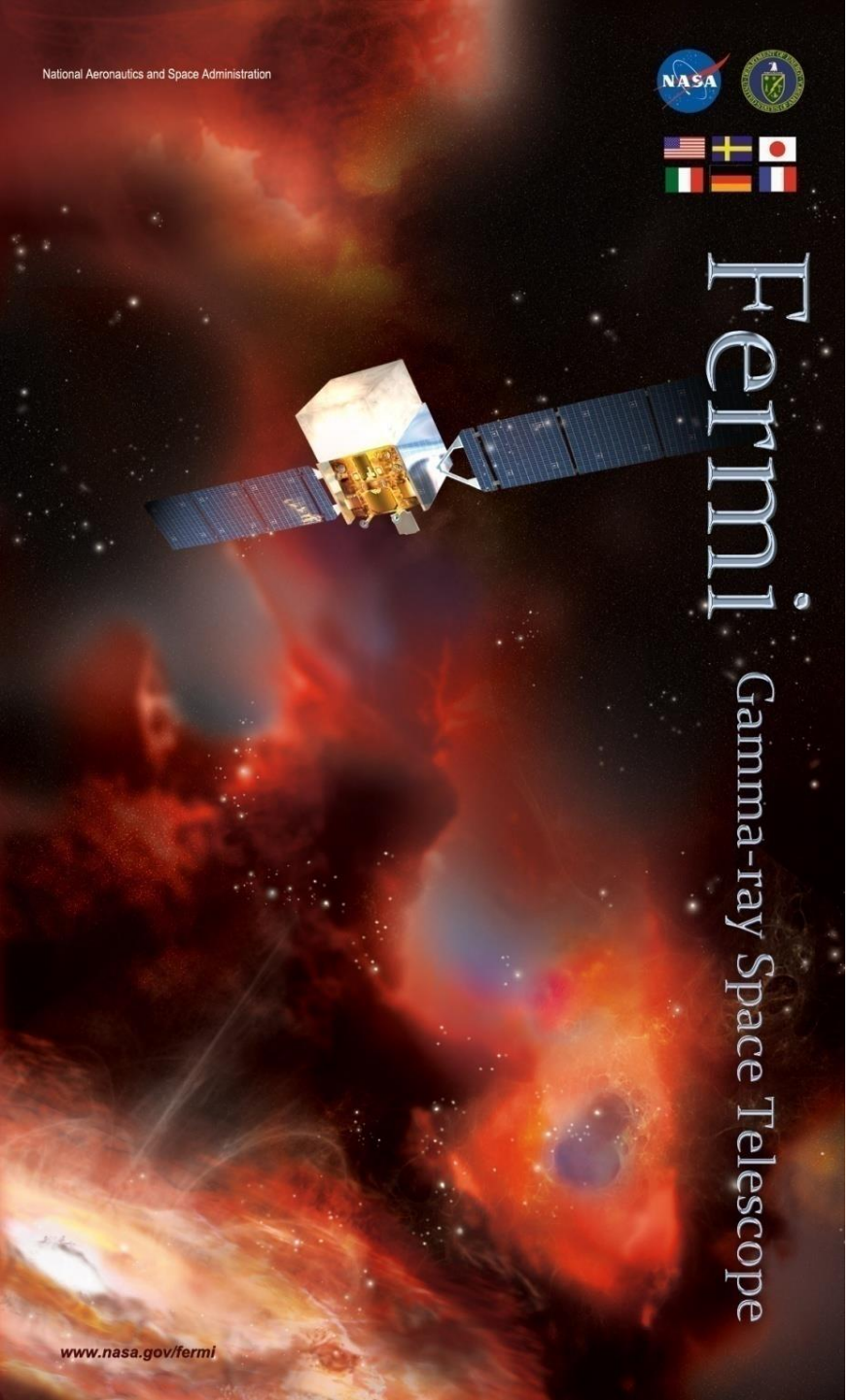

Study of periodicity in Blazar light curves observed by *Fermi*-LAT

Author:
Paolo Cristarella Orestano [1,2]

Supervisors:
Prof. Gino Tosti [1,2], Dr. Sara Cutini [2], Dr. Stefano Germani [1,2]

[1] University of Perugia
[2] INFN Perugia

Index

- Blazar classification
  - Blazar variability and periodicity
- Sources selection
- Analysis methods
  - Weighted Wavelet Z-transform
  - Lomb Scargle Periodogram
  - False Alarm Probability
  - Time series and red noise simulations
- Analysis results
- Conclusions

Blazar classification

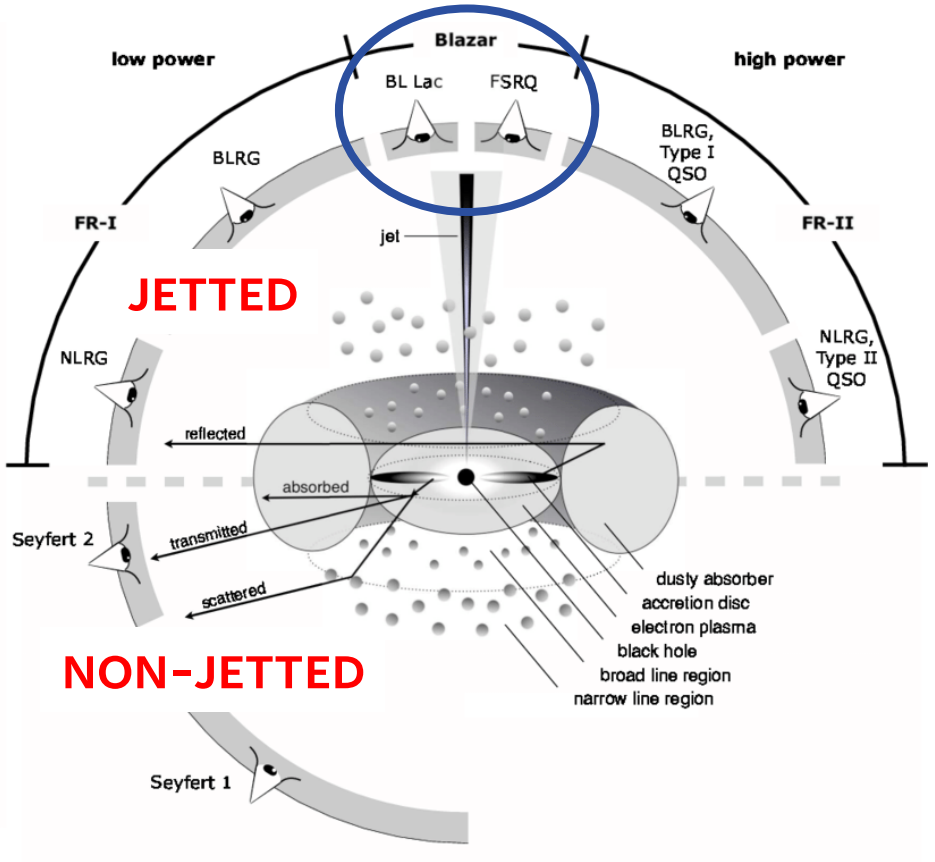

Blazar classification

Flat Spectrum Radio Quasar (FSRQ)

High Luminosity:

10^{46} - 10^{48} erg/s

Collimated jets

with hot spots

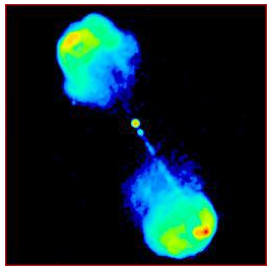

3C 47

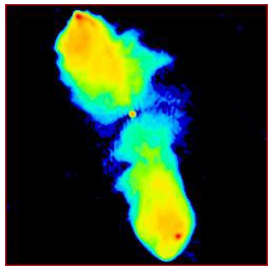

3C 98

BL Lac object (BLL)

Low Luminosity:

10^{45} - 10^{46} erg/s

Widespread jets

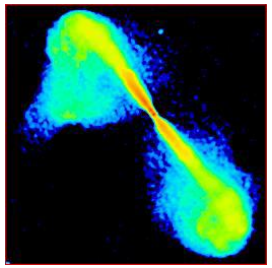

3C 296

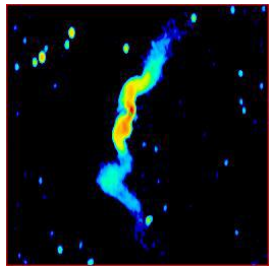

3C 31

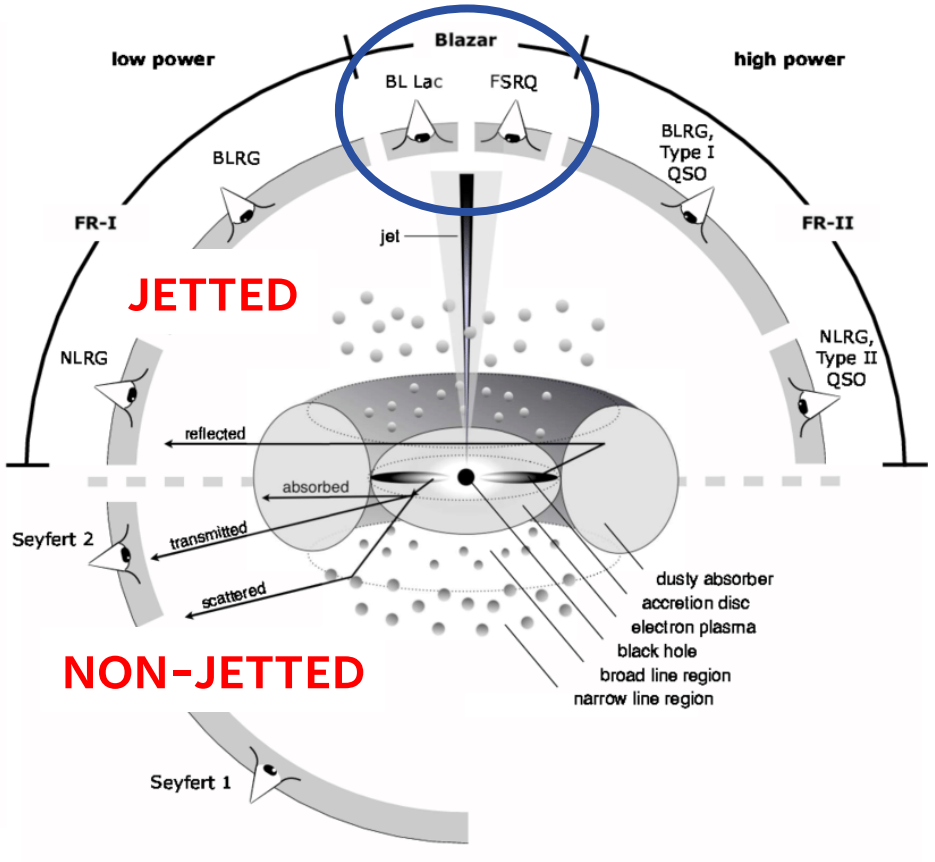

Blazar classification

Flat Spectrum Radio Quasar (FSRQ)

Flat spectrum and emitting lines

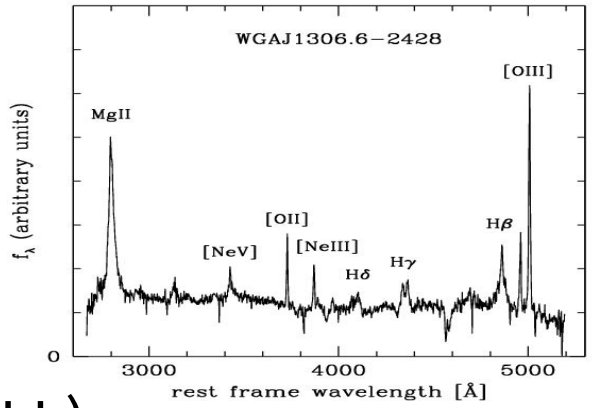

BL Lac object (BLL)

No emitting lines

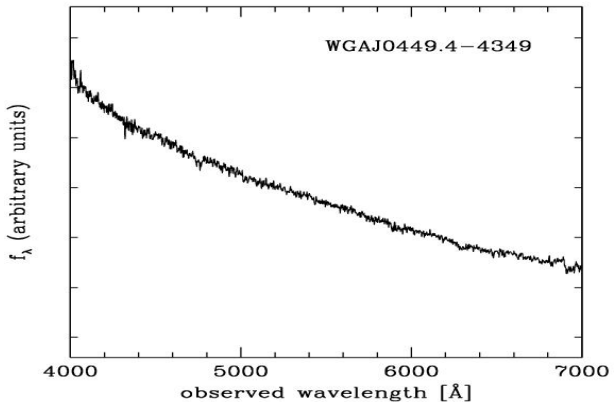

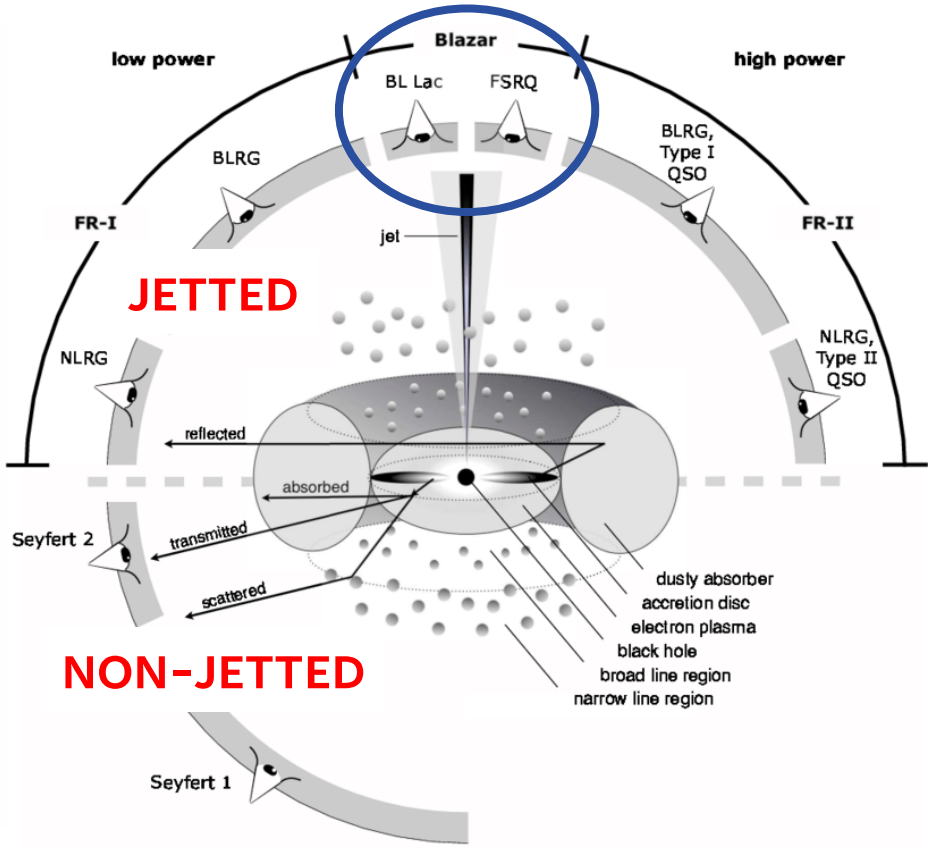

Blazar variability

Large variability at various wavelengths.

Red noise type power spectrum $\propto 1/f^{\delta}$. The parameter δ goes from flicker noise (δ=1) to Brownian noise (δ=2).

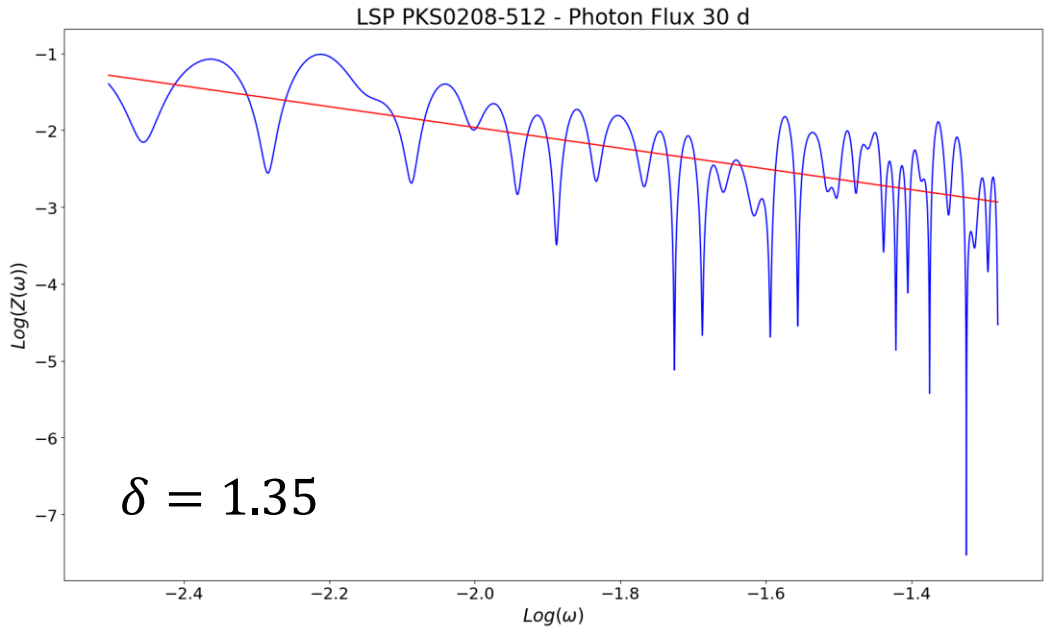

3C 279

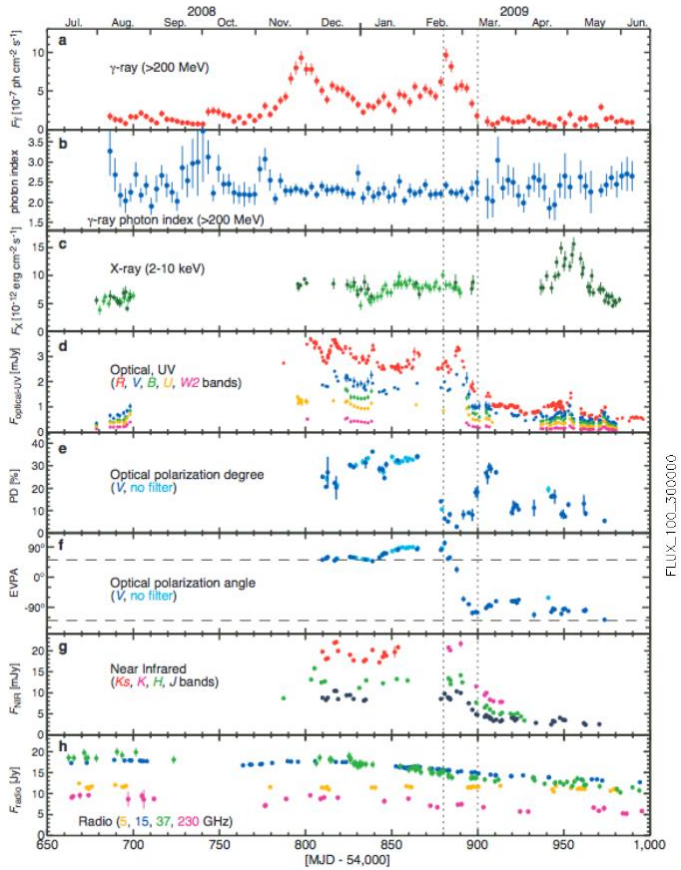

https://doi.org/10.1038/nature08841

Blazar periodicity

Long-term periodicity could be related to binary black holes [1]:

- Intensity modulation by Doppler factor.
- Precession, deflection or curvature of the jet changing the viewing angle.

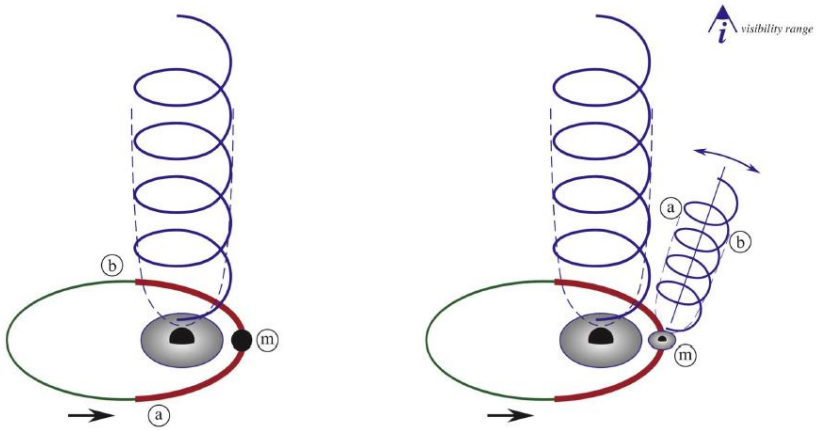

From Tavani et al., 2018 [2]

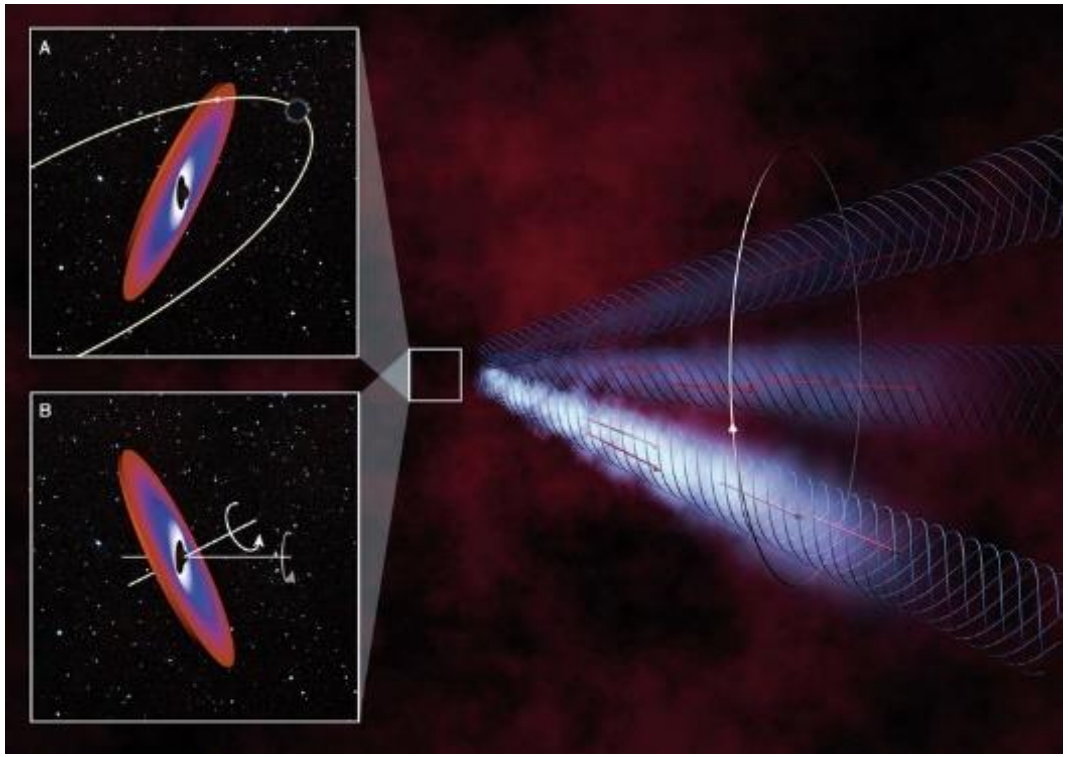

Source selection

From the Light Curve Repository[1] 1525 γ-ray sources analyzed: 571 FSRQ, 476 BLL, 371 unkown types of blazars, 107 other sources.

Six light curves data types: Energy flux (free index), Photon Flux (fixed index), 30d, 7d and 3d sampling.

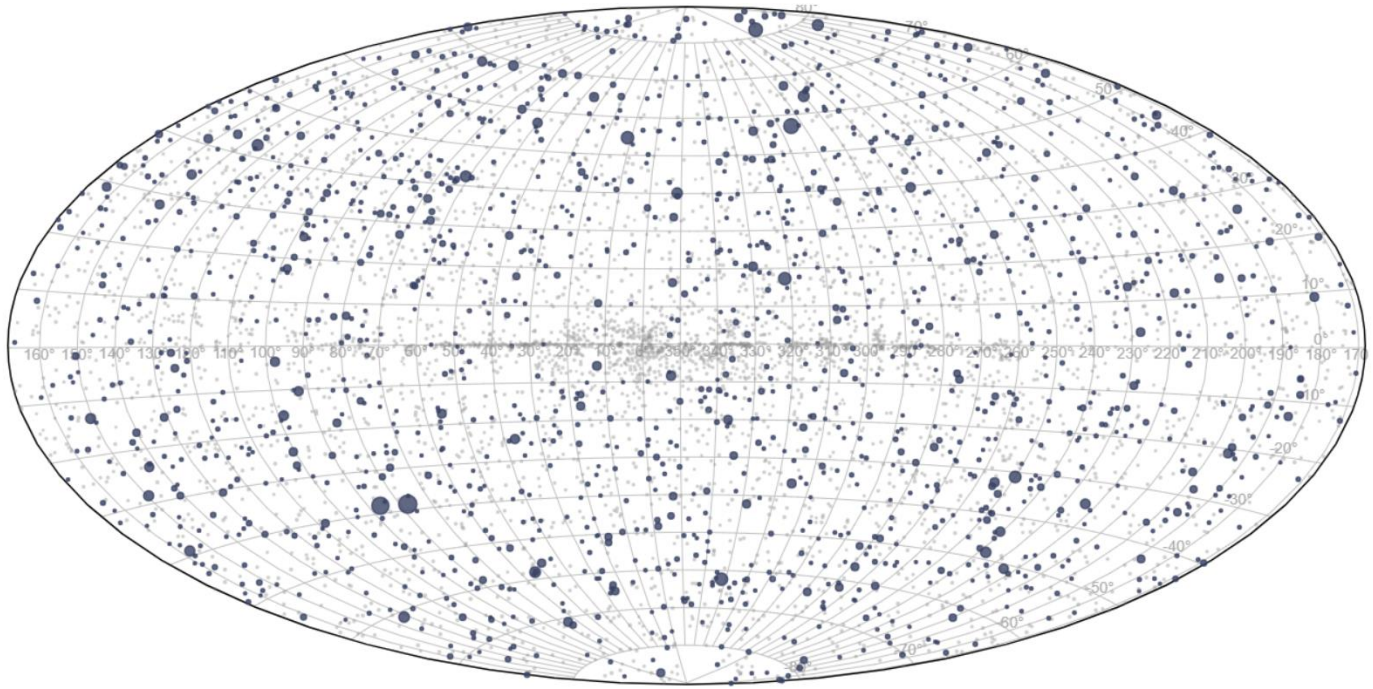

[1] https://fermi.gsfc.nasa.gov/ssc/data/access/lat/LightCurveRepository/

Weighted Wavelet Z-transform (WWZ)

Time series projection onto a model function (Morlet) [3].

Detects transient periodicities, studies temporal evolution of data and signal parameters.

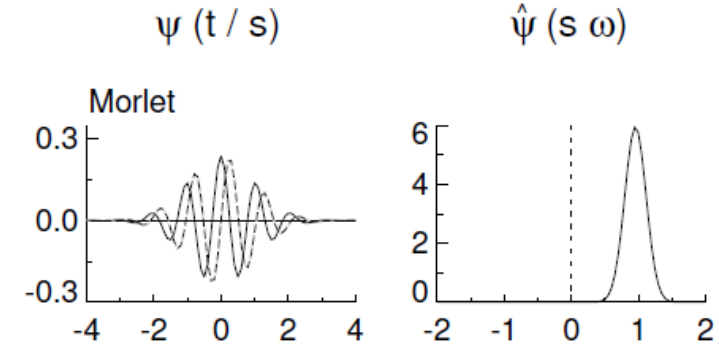

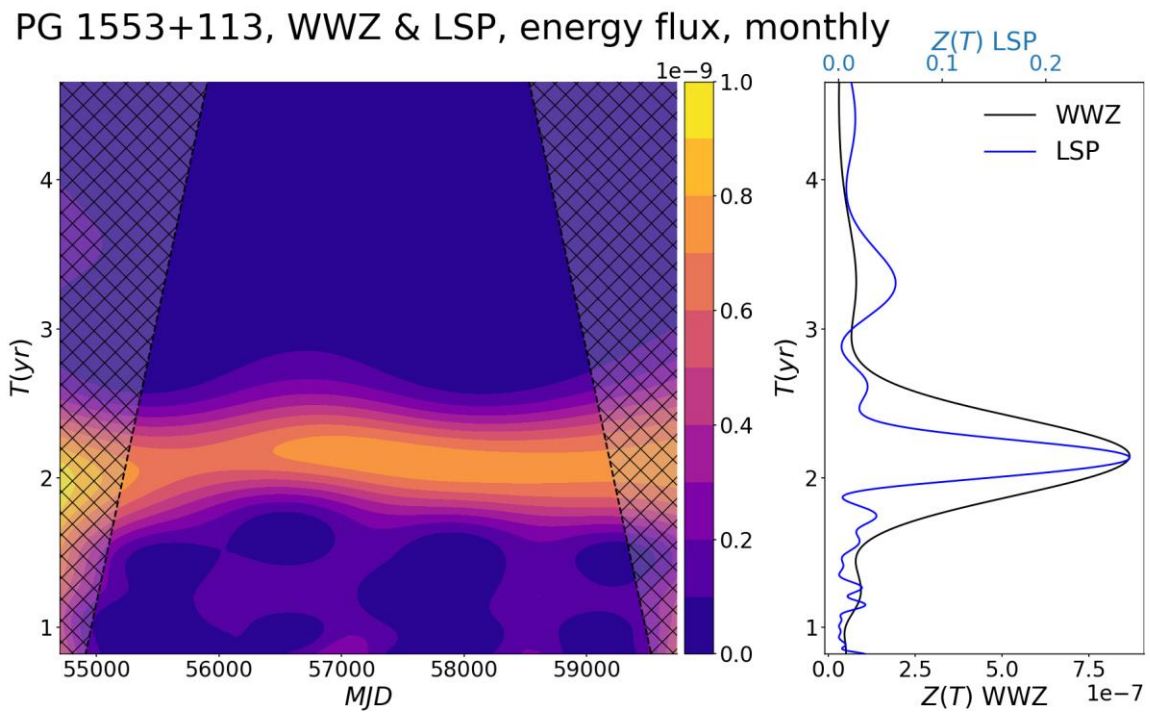

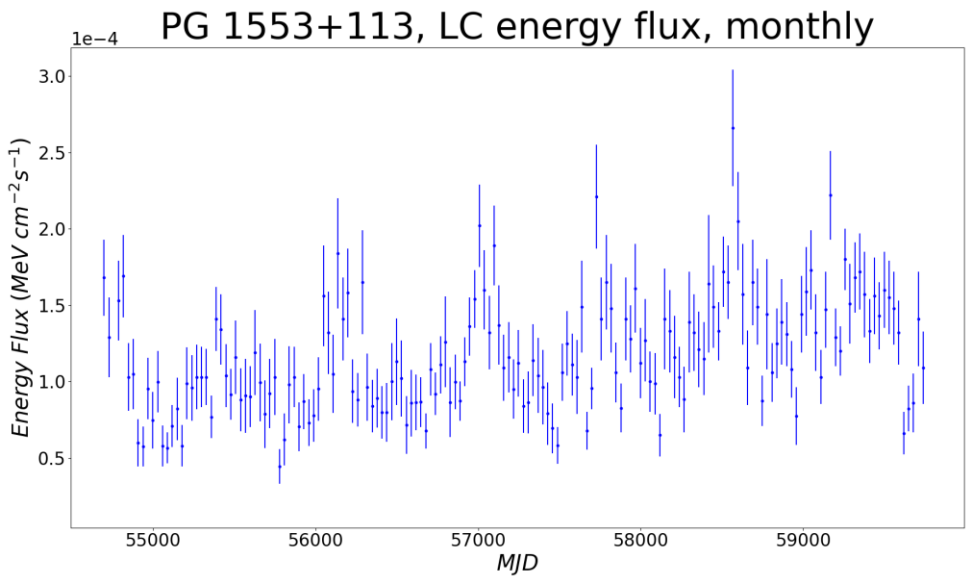

Lomb-Scargle Periodogram (LSP)

Square module of the Discrete Fourier transform. In addition to the changes by Scargle [4] we take into account some consideration by Vanderplas [5].

Not precision but significance:

The number of points N and the signal-to-noise ratio S/N do not affect the width of the peak but only its height.

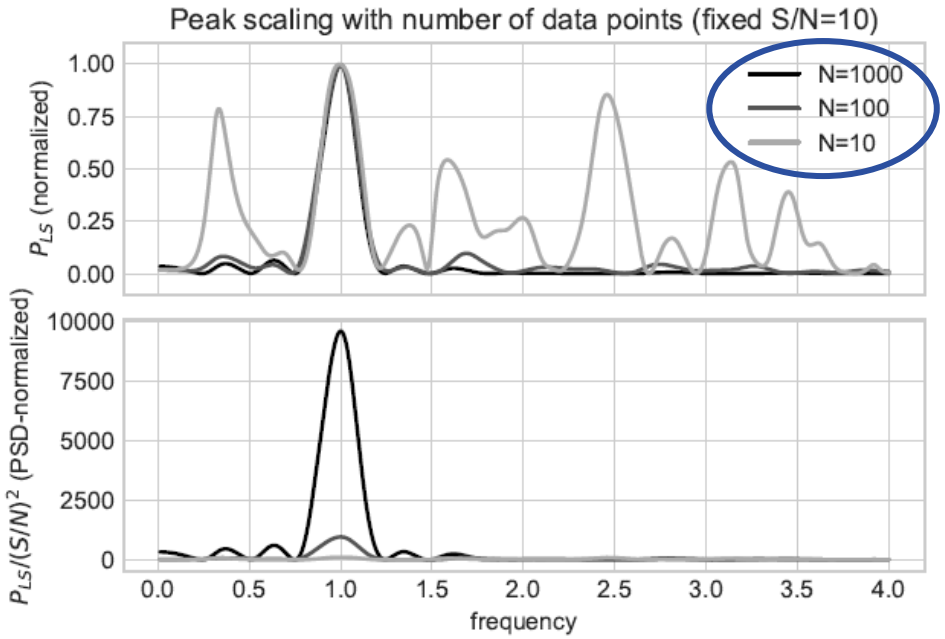

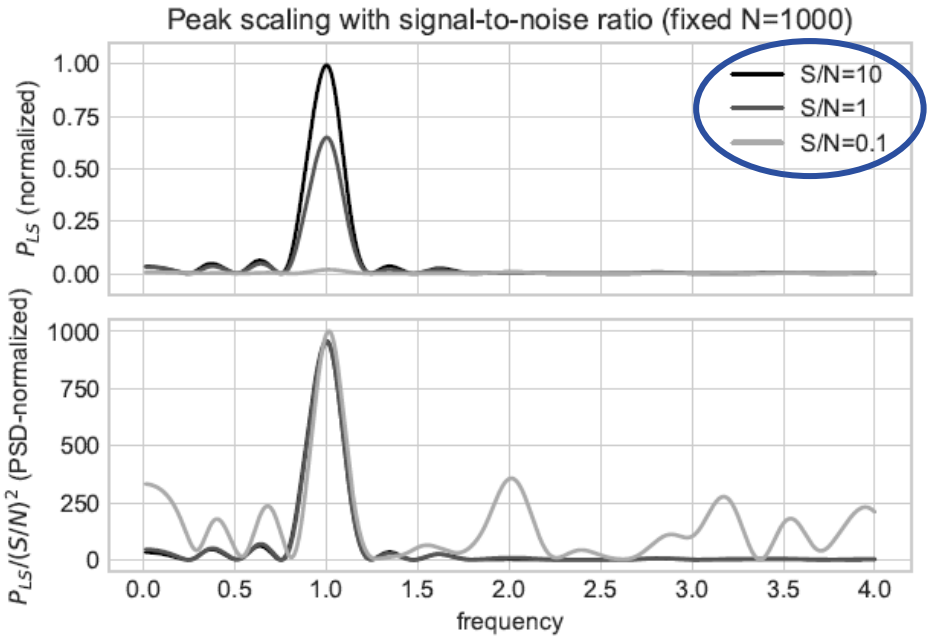

False Alarm Probability (FAP)

To compare peak height with background and spurious peaks.

Probability that a peak of a certain height Z will be found from a data set consisting of white noise.

- **Naive**

  The cumulative probability of observing a value less than Z with white noise is $P(Z) = 1 - e^{-Z}$.

$$FAP_{Naive}\,(Z) = 1 - \big(P(Z)\big)^{N_{eff}}$$

- **Bootstrap**

  Randomization of the time series, high computational cost. Simulations required: N=10/r.

- **Baluev**

  Extreme value theory for random processes. Upperbound for the FAP.

False Alarm Probability (FAP)

Naive method overestimates the significance, while Baluev method underestimates it.
From the FAP we extrapolate a fictitious number of σ.

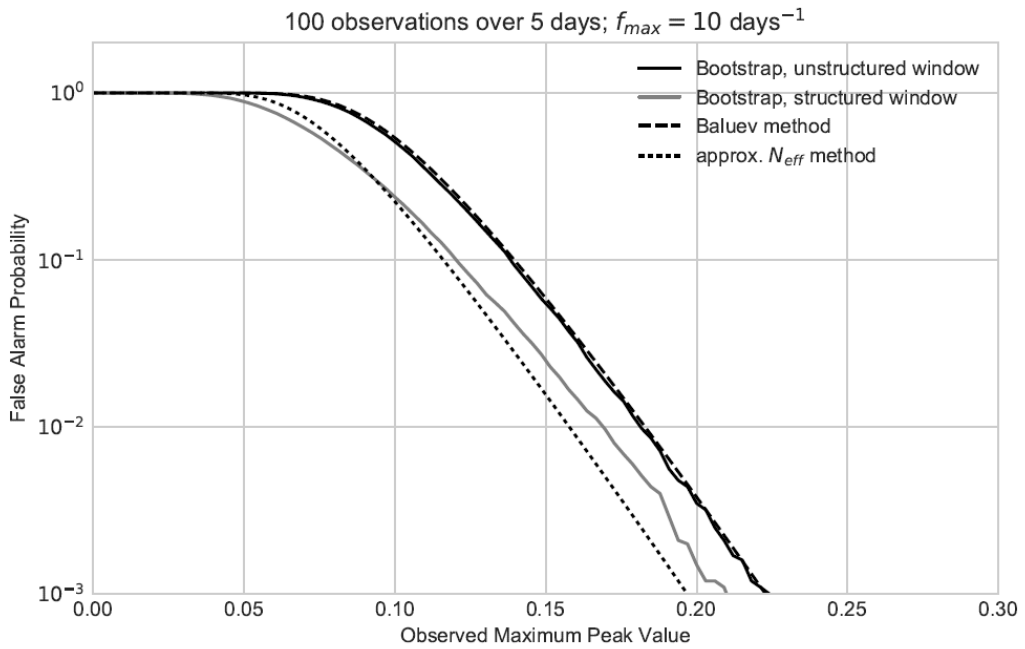

From Vanderplas [5]

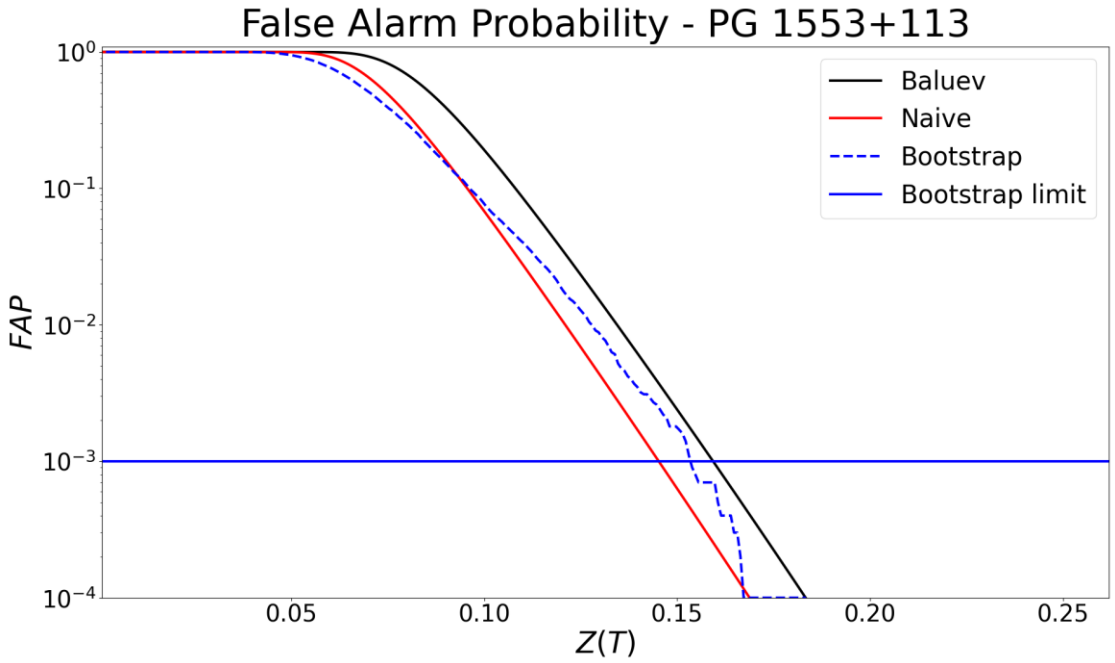

Time series and red noise simulations

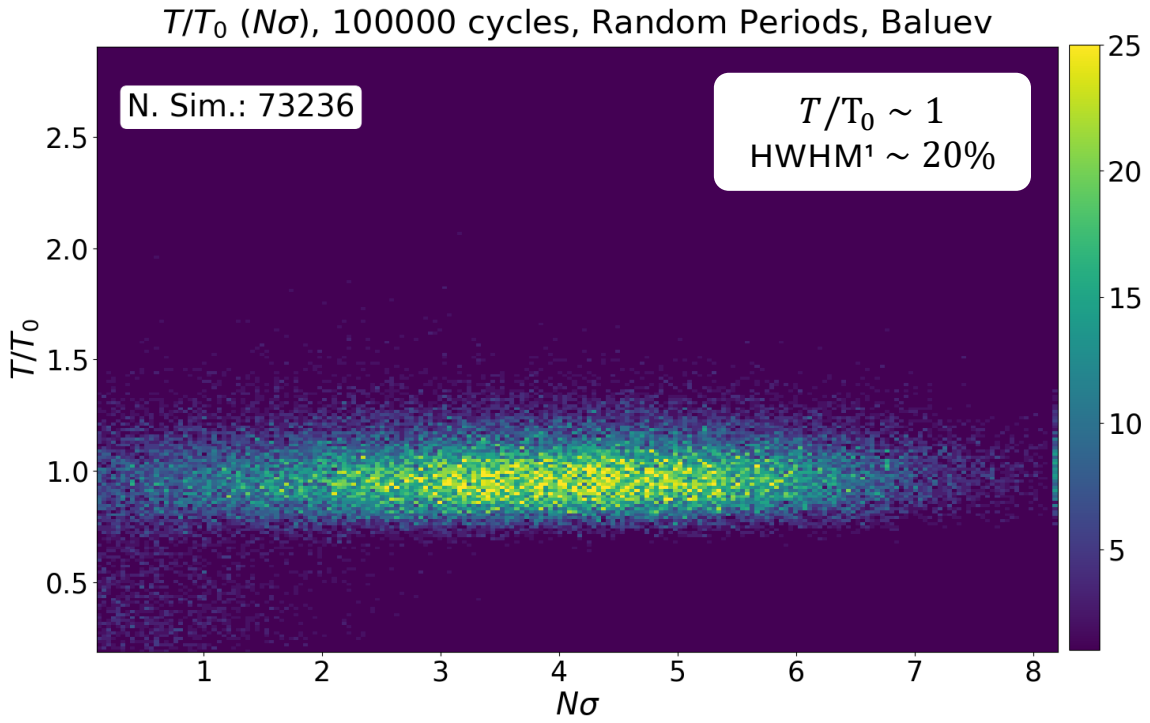

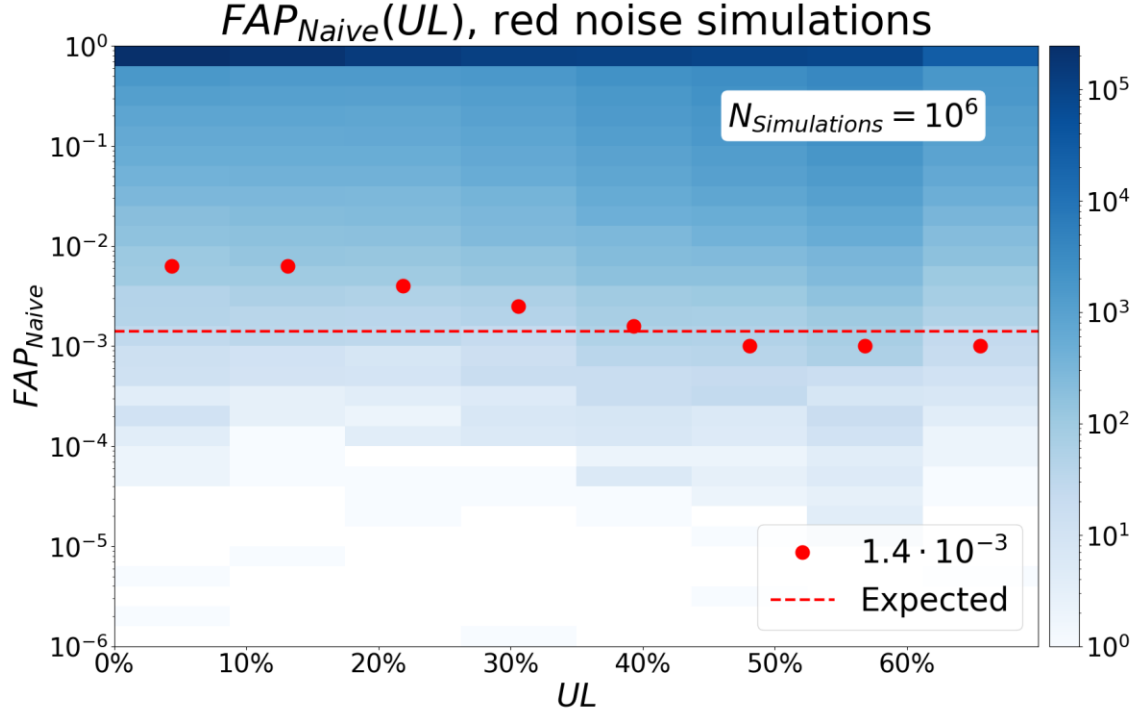

[1] Half Width at Half Maximum

Analysis results

Significant periodicities found in 23 blazars: 13 FSRQ and 10 BLL; many data types, $> 3\sigma$, and Normalized Root Mean Square Deviation NRMSD $< 3\%$; boundary of 40% UL.

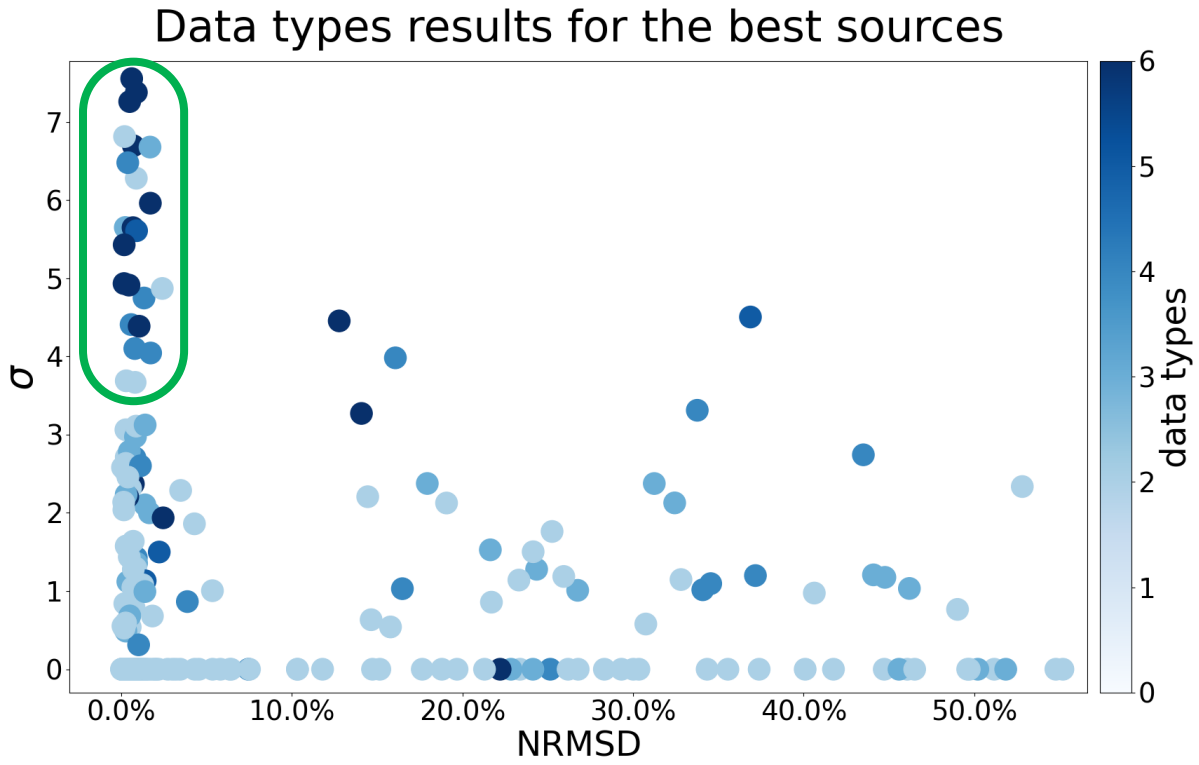

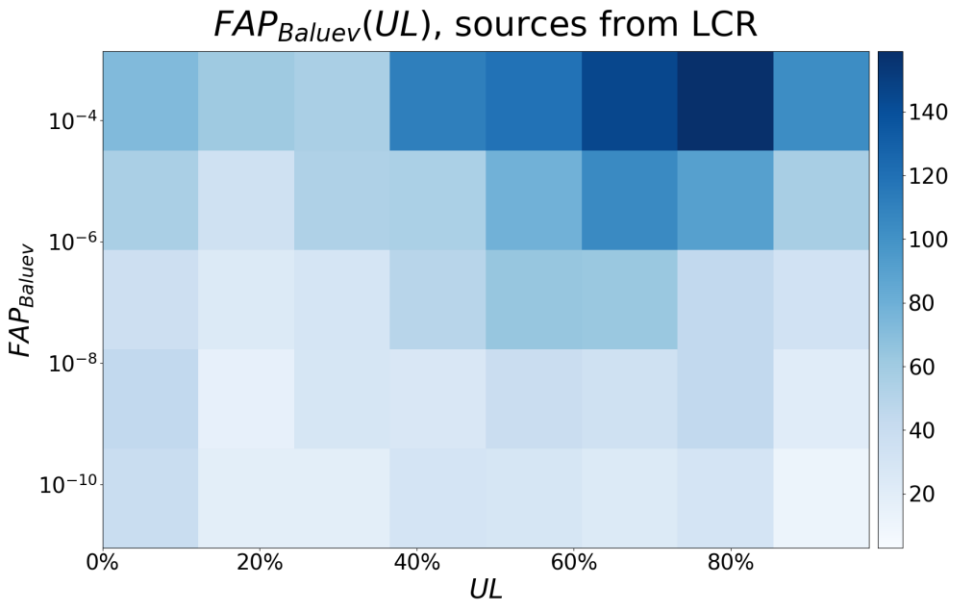

Analysis results

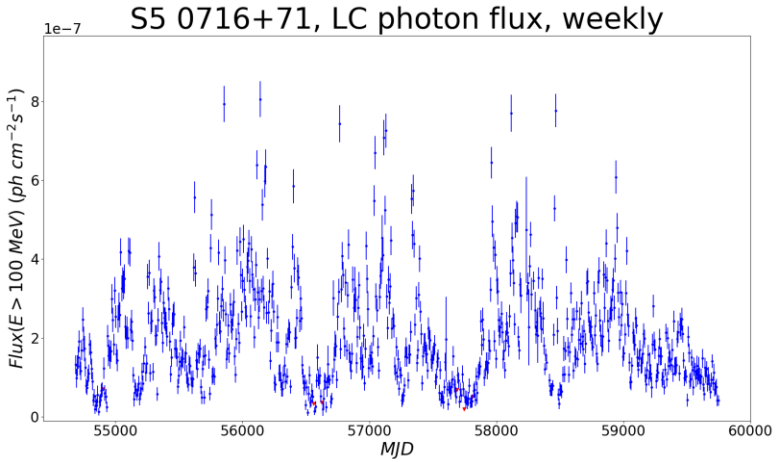

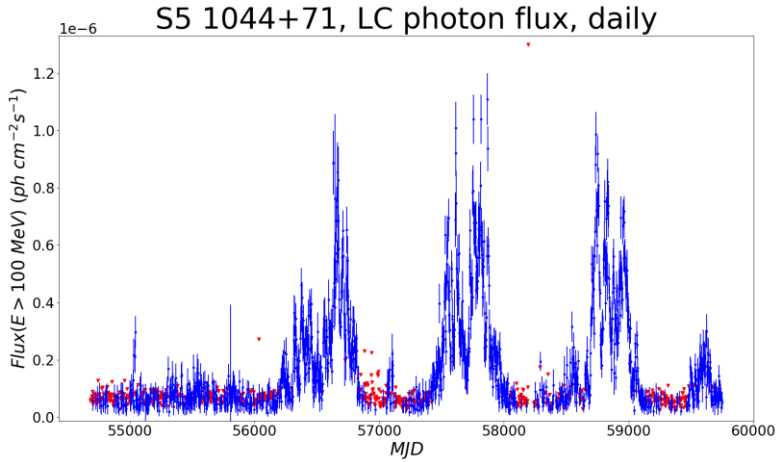

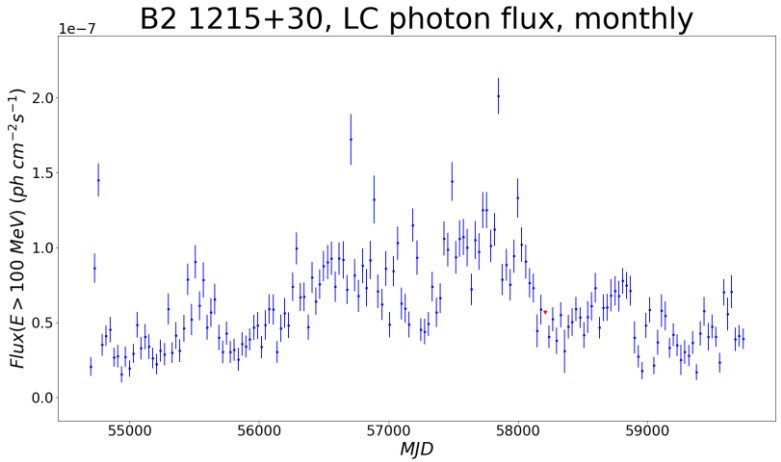

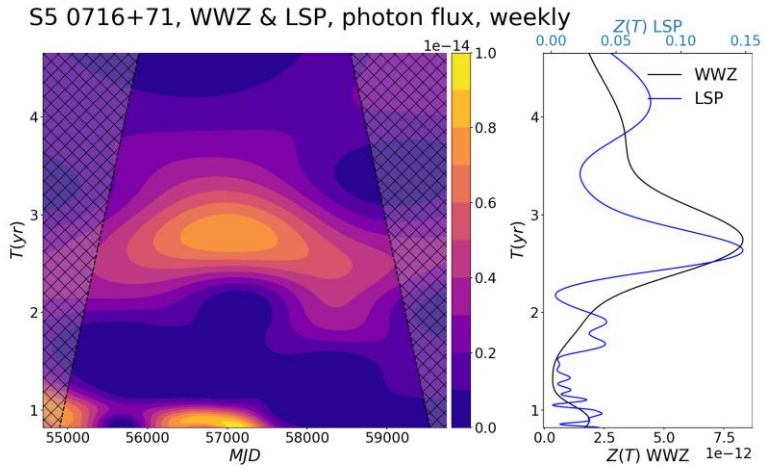

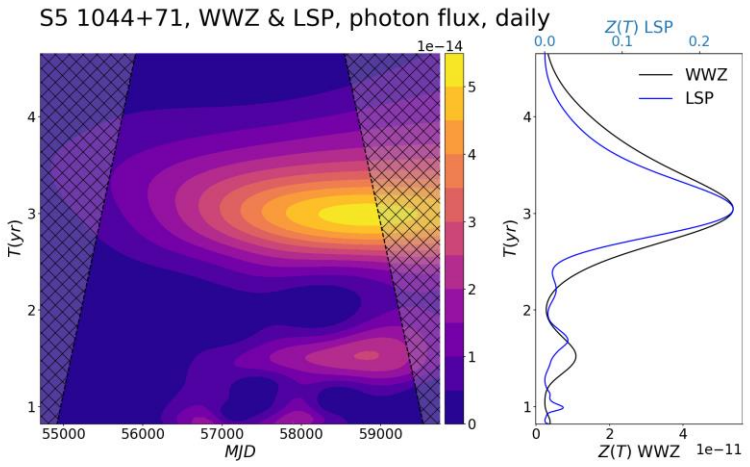

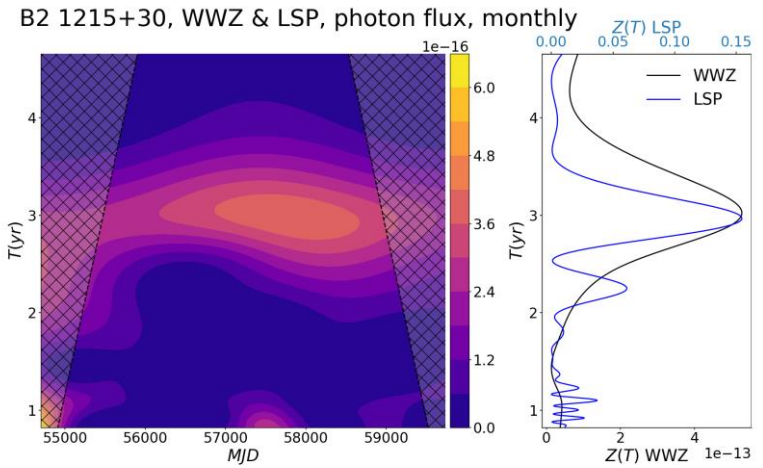

Conclusions

- Significant periodicities in 23 blazars. With a golden sample of 6 sources.
- The analysis method was validated through periodic light curve simulations, and with red noise simulations the significance estimation.
- A suitable model has yet to be found.

Source Name	RA J2000	Dec J2000	Type	Best Period (yr)	Nσ
TXS 0059+581	15.701	58.409	FSRQ	4.3	5σ
PKS 0208-512	32.695	−51.022	FSRQ	3.9	5σ
MG1 J021114+1051	32.809	10.857	BLL	4.1	4σ
4C +28.07	39.474	28.804	FSRQ	3.8	$> 5\sigma$
PKS 0405-385	61.763	−38.439	FSRQ	2.7	3σ
PKS 0426-380	67.173	−37.941	BLL	3.5	$> 5\sigma$
PKS 0454-234	74.261	−23.414	FSRQ	3.5	$> 5\sigma$
TXS 0506+056	77.359	5.701	BLL	3.0	5σ
TXS 0518+211	80.445	21.213	BLL	3.1	5σ
OG 050	83.172	7.549	FSRQ	3.0	4σ
S5 0716+71	110.489	71.341	BLL	2.6	$> 5\sigma$
OJ 014	122.861	1.776	BLL	4.2	5σ
S4 0814+42	124.557	42.382	BLL	2.2	4σ
S5 1044+71	162.107	71.730	FSRQ	3.0	$> 5\sigma$
S4 1144+40	176.74	39.977	FSRQ	3.3	$> 5\sigma$
Ton 599	179.884	29.245	FSRQ	3.6	5σ
B2 1215+30	184.476	30.118	BLL	3.0	$> 5\sigma$
4C +21.35	186.228	21.381	FSRQ	4.1	5σ
PKS 1502+106	226.103	10.498	FSRQ	2.3	5σ
B2 1520+31	230.545	31.739	FSRQ	2.9	5σ
PG 1553+113	238.932	11.188	BLL	2.2	$> 5\sigma$
PKS 2155-304	329.714	−30.225	BLL	1.7	3σ
PKS 2326-502	352.329	−49.932	FSRQ	3.1	3σ

Bibliography

[1] S. Komossa, "*Observational evidence for binary black holes and active double nuclei*", Memorie della Società Astronomica Italiana, vol. 77, p. 733, 2006.

[2] M. Tavani, Marco, et al. "*The blazar PG 1553+ 113 as a binary system of supermassive black holes*" , ApJ 854.1 (2018): 11.

[3] G. Foster, "*Wavelets for period analysis of unevenly sampled time series*", AJ, vol. 112, pp. 1709–1729, Oct. 1996

[4] J. D. Scargle, "Studies in astronomical time series analysis. II. Statistical aspects of spectral analysis of unevenly spaced data", ApJ, vol. 263, pp. 835–853, Dec. 1982.

[5] J. T. VanderPlas, "*Understanding the Lomb-Scargle Periodogram*", ApJS, vol. 236, p. 16, May 2018.

[6] M. Ackermann, et al., "*Multiwavelength evidence for quasi-periodic modulation in the gamma-ray blazar pg 1553+113*", The Astrophysical Journal, vol. 813, p. L41,Nov 2015.

[7] P. Peñil, et al., "*Systematic Search for γ-Ray Periodicity in Active Galactic Nuclei Detected by the Fermi Large Area Telescope*", ApJ, vol. 896, p. 134, June 2020.

Backup slides

Models

Instability in accretion flux. The magnetic field make the accretion flux asymmetric.

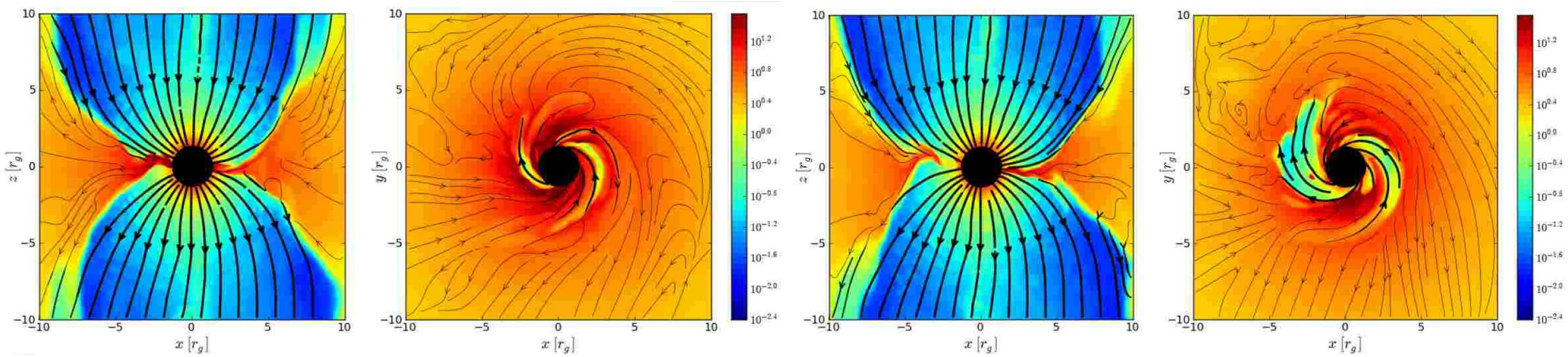

Models

Strong and turbulent magnetic fields may cause precession, rotation or helical structure of jets, or periodic changes of the Doppler factors.
Jet precession and rotation due to the presence of rigid and massive body in the accretion disk.

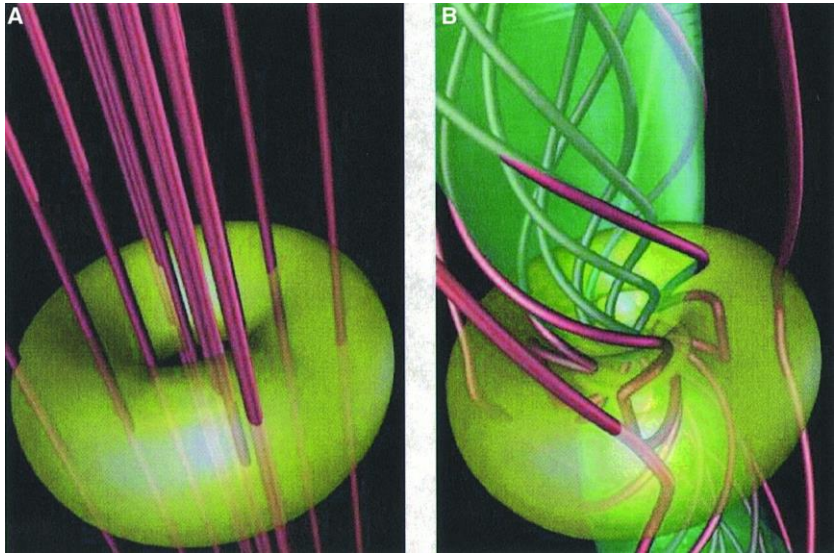

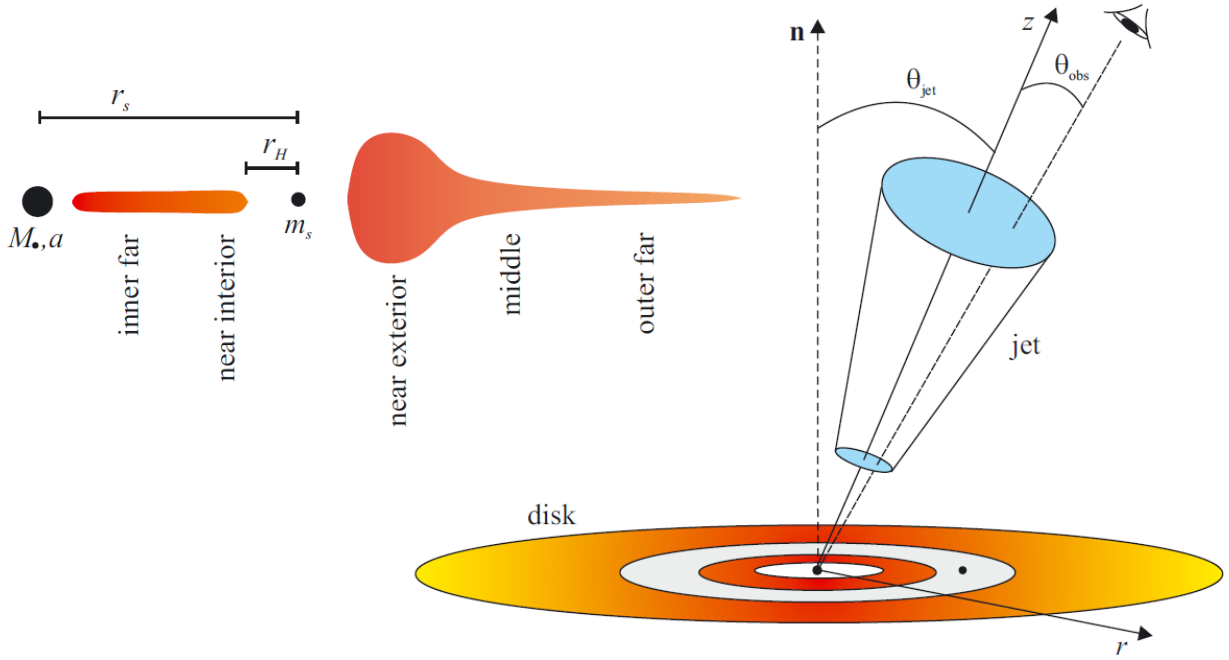

Weighted Wavelet Z-transform (WWZ)

Considering the Morlet as mother function we define the model function for the projection:

$$y(t) = \sum_a^M y_a F_a(t)$$

$S_{ab} = \langle F_a | F_b \rangle$, in order to determine y_a coefficients for the best-fit of the mother function on the time series x:

$$y_a = \sum_b S_{ab}^{-1} \langle F_b | x \rangle$$

Statistic weights w_i to have a weighted projection:

$$\langle F | x \rangle = \frac{\sum_\alpha w_\alpha F(t_\alpha) x(t_\alpha)}{\sum_\beta w_\beta}$$

We define WWZ as:

$$Z_W = \frac{(N_{eff} - 3) V_y}{2(V_x - V_y)}$$

Where $\mathrm{N_{eff}} = (\sum w_\alpha)^2 / \sum w_\alpha^2$.

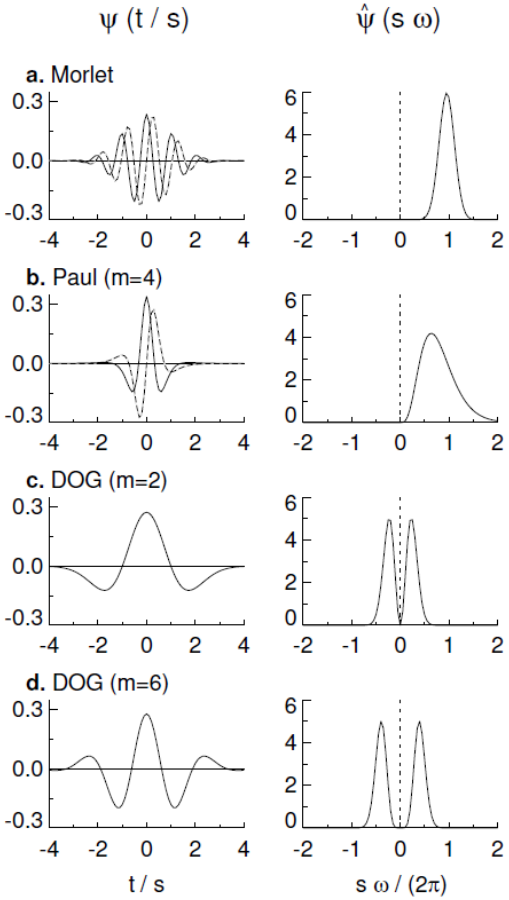

Weighted Wavelet Z-transform (WWZ)

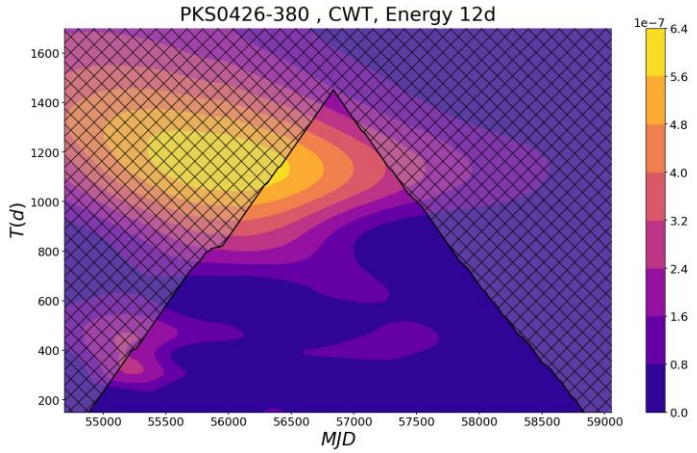

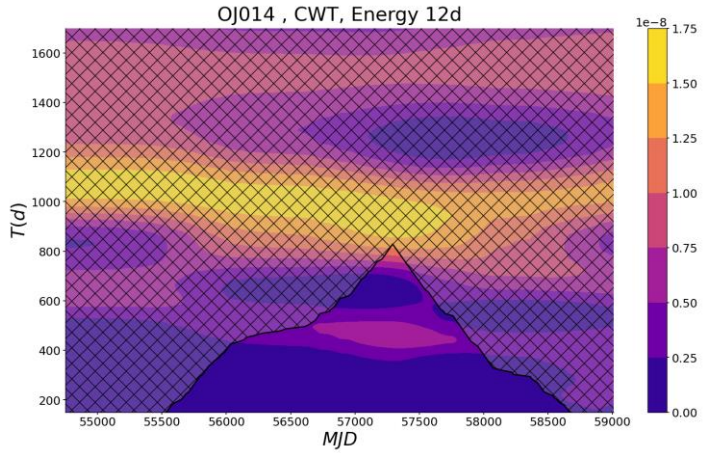

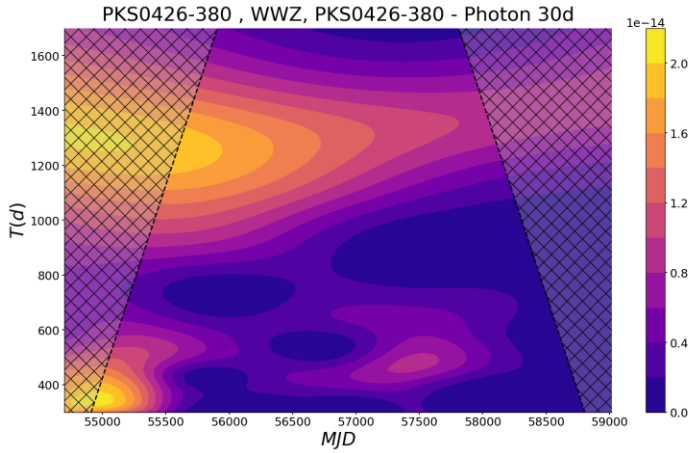

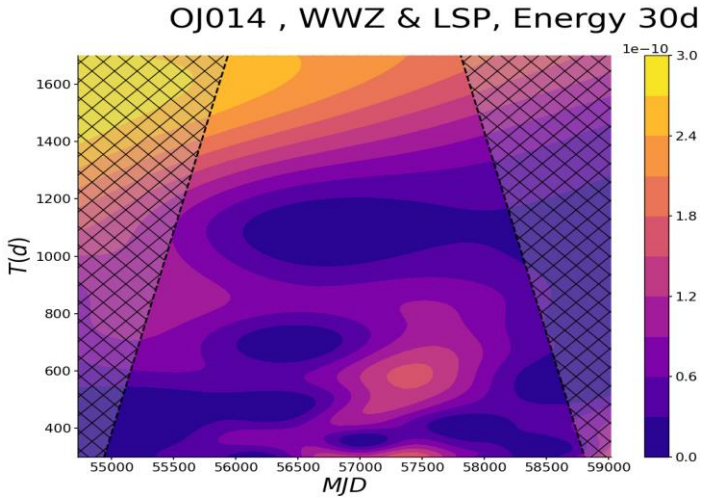

Lomb-Scargle Periodogram (LSP)

Signal and noise: $X_j = X(t_j) = X_{S\,j} + R_j$, (j = 1, … , N).

Classic periodogram: $P_X(\omega) = \frac{1}{N}|DFT_X(\omega)|^2 = \frac{1}{N}\left|\sum_{j=1}^{N} X(t_j)e^{-i\omega t_j}\right|^2$

Not useful in case of noisy data. Spectral Leakage.

Discrete Fourier Transform:

$$DFT_X(\omega) = \sqrt{N/2}\sum_{j=1}^{N} X(t_j)(A(\omega)\cos\omega t_j + iB(\omega)\sin\omega t_j)$$

If $A(\omega) = B(\omega) = \sqrt{2/N}$ we obtaing the classic periodogram. Lomb-Scargle changes:

$$A(\omega) = \left(\sum_j \cos^2\omega t_j\right)^{-1/2} \quad ; \quad B(\omega) = \left(\sum_j \sin^2\omega t_j\right)^{-1/2}$$

Modified periodogram:

$$P_X(\omega) = \frac{1}{2}\left(\frac{\left(\sum_j X_j \cos\omega(t_j-\tau)\right)^2}{\sum_j X_j \cos^2\omega(t_j-\tau)} + \frac{\left(\sum_j X_j \sin\omega(t_j-\tau)\right)^2}{\sum_j X_j \sin^2\omega(t_j-\tau)}\right) \quad \text{with} \quad \tan 2\omega\tau = \frac{\sum_j \sin 2\omega t_j}{\sum_j \cos 2\omega t_j}$$

Baluev FAP

Two hypothesis: noise H and periodic signal K. FAP comes from the probability distribution of maxima in periodograms under H hypothesis.

Least-squares periodogram:

$$z(f) = \frac{\chi_H^2 - \chi_K^2(f)}{2}$$

With the theory of random processes we estimate the FAP:

$$FAP_{Baluev}(z, f_{max}) = 1 - \exp(-We^{-z}\sqrt{z}\,)$$

$$W = f_{max}T_{eff} \quad ; \quad T_{eff} = \sqrt{4\pi Dt} \quad ; \quad Dt = \overline{t^2} - \bar{t}^2$$

Time series simulations

$$X_{sim}(t) = \begin{cases} g(t) = A\sin(t\omega_0 + \phi_0) + h + a_0 e^{-\left(\frac{t-b_0}{c_0}\right)^2}, & g(t) > w(t) \\ w(t), & g(t) < w(t) \\ upperlimit, & g(t), w(t) < UL_0 \end{cases}$$

With $w(t)$ white noise. Parameters with 0 wary for each simulation, while A and h vary randomly in short range over the observation time.

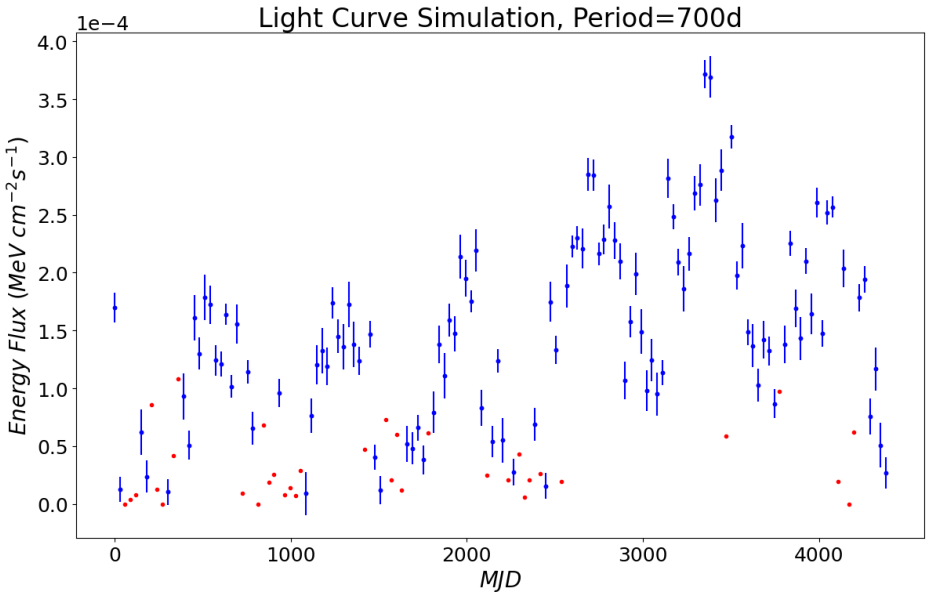

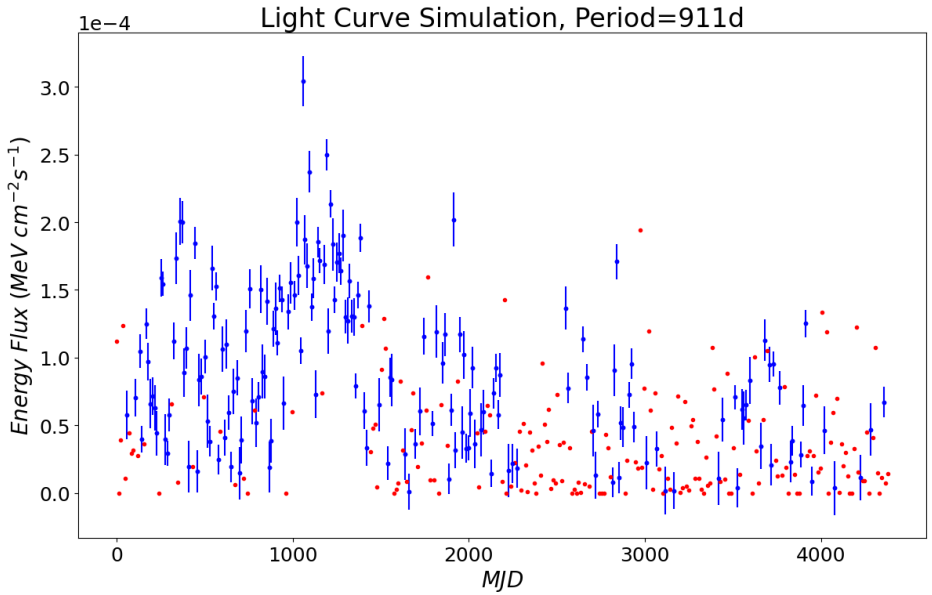

Relativistic beaming effect

Blazar when the viewing angle is $\theta \leq 1/\Gamma$, Doppler beaming with Lorentz factor $\Gamma \approx 10 - 20$.

Kinematic Doppler factor:

$$\delta = \left(\gamma(1 - \beta \cos\theta)\right)^{-1}$$

Flux transformation with Doppler factor:

$$F_\nu(\nu) = \delta^{3+\alpha} F'_{\nu'}(\nu)$$

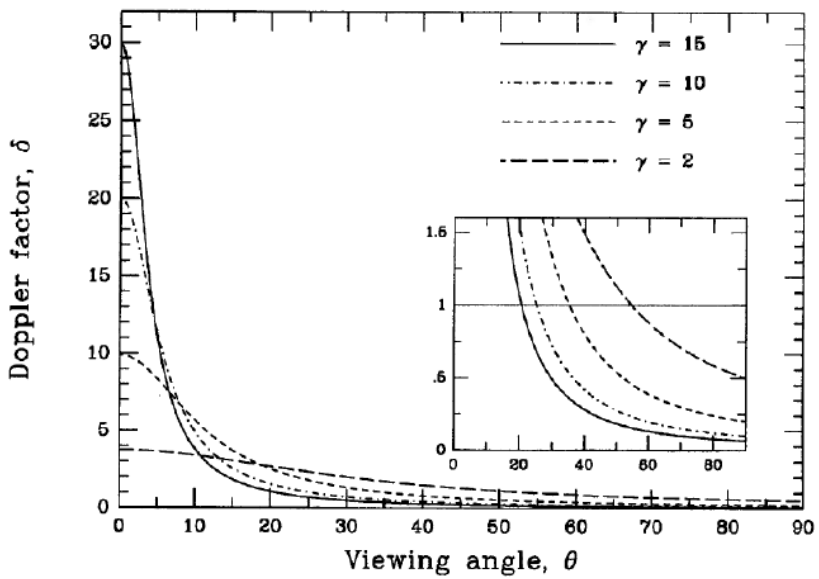

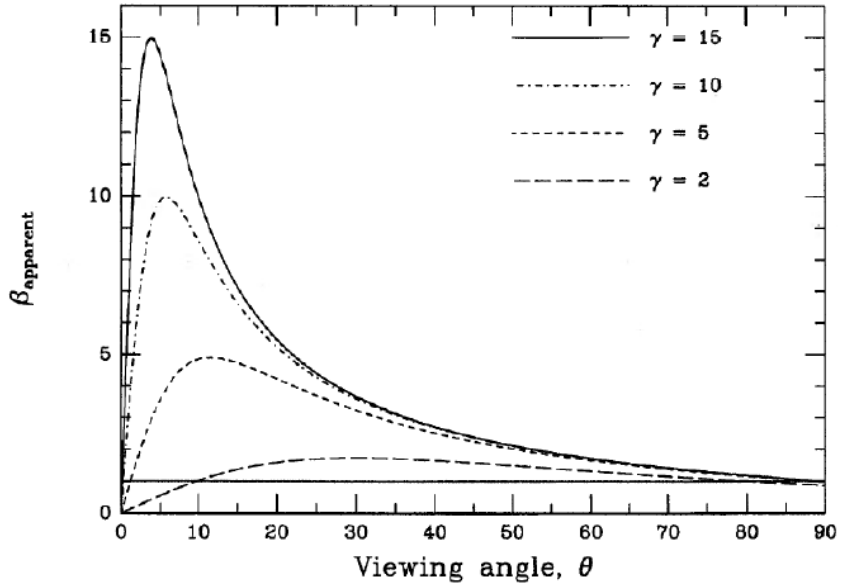

More results

PKS 0426-380, LC photon flux, monthly

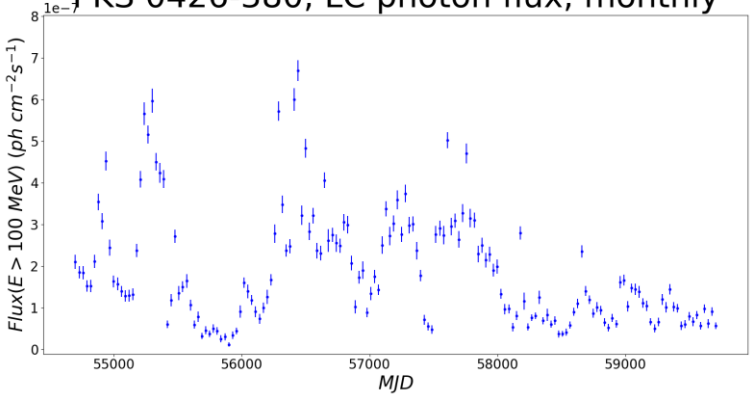

PKS 0454-234, LC photon flux, monthly

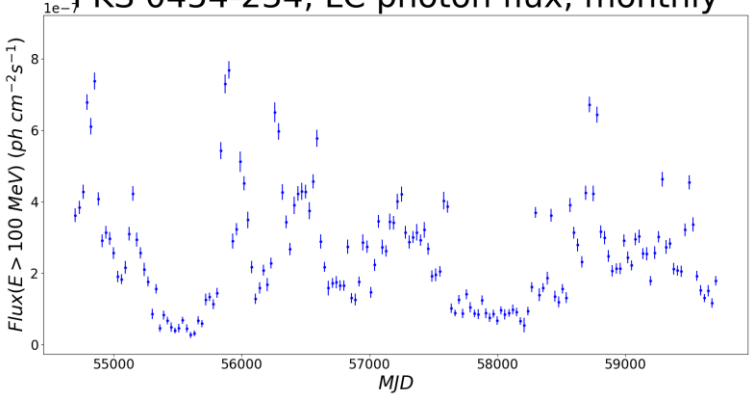

TXS 0518+211, LC photon flux, monthly

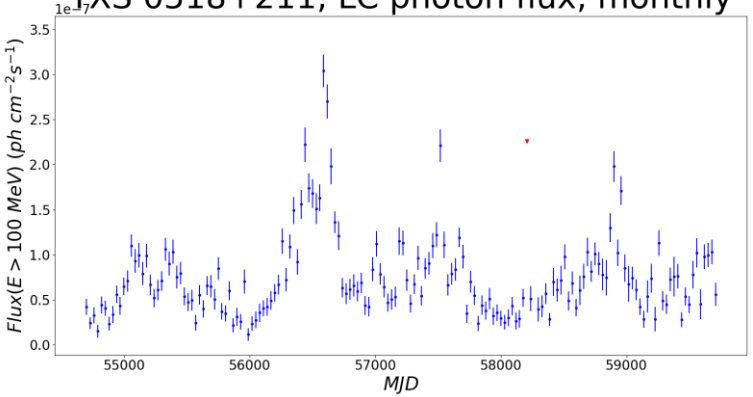

PKS 0426-380, WWZ & LSP, photon flux, monthly

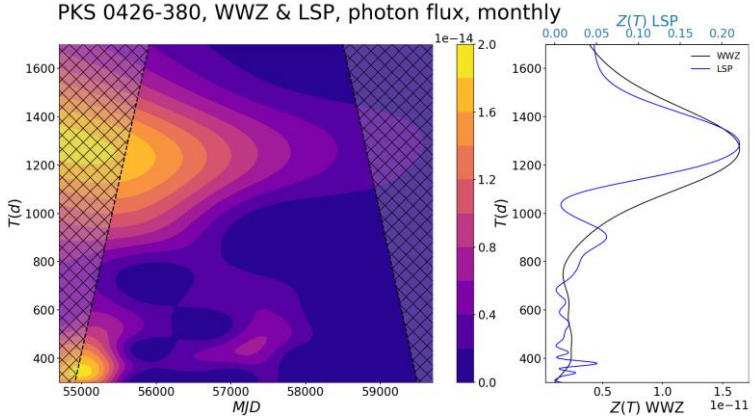

PKS 0454-234, WWZ & LSP, photon flux, monthly

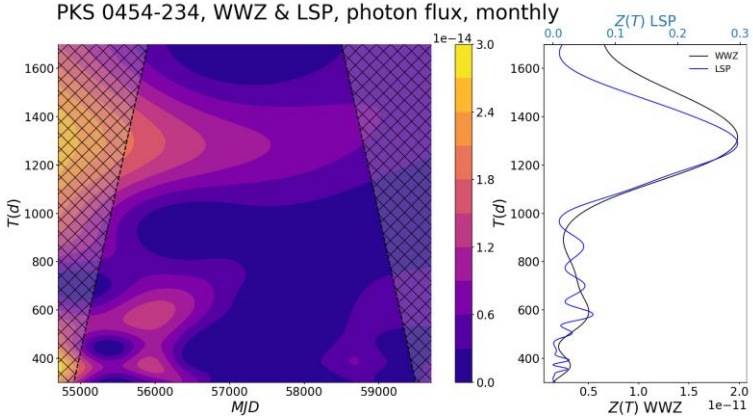

TXS 0518+211, WWZ & LSP, photon flux, monthly

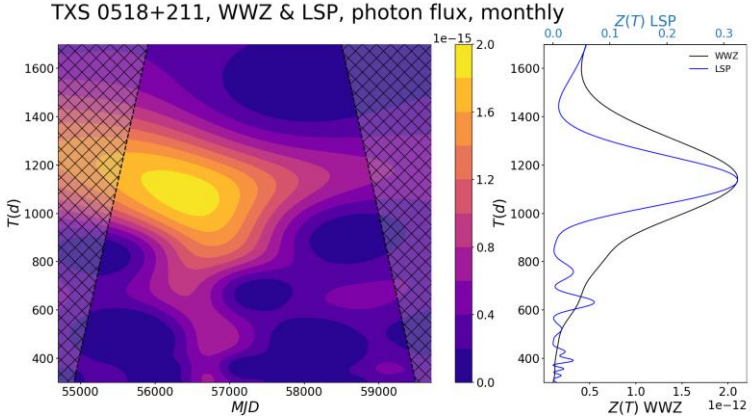

More results

PKS 0405-385, LC energy flux, monthly

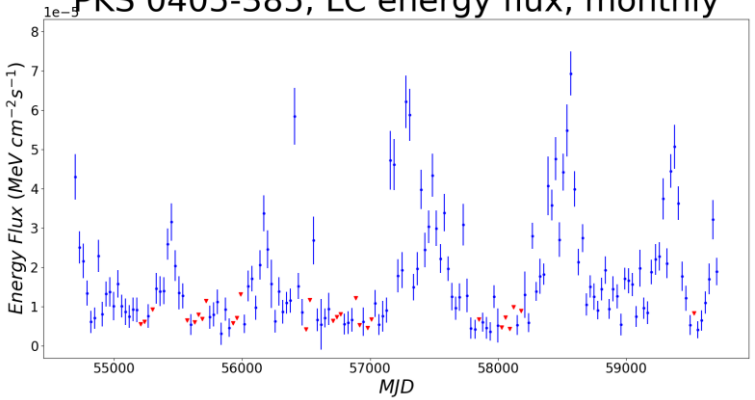

OJ 014, LC photon flux, monthly

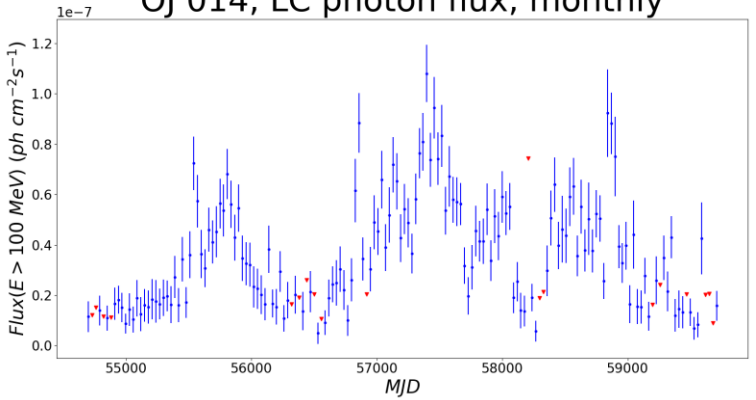

PKS 2155-304, LC energy flux, monthly

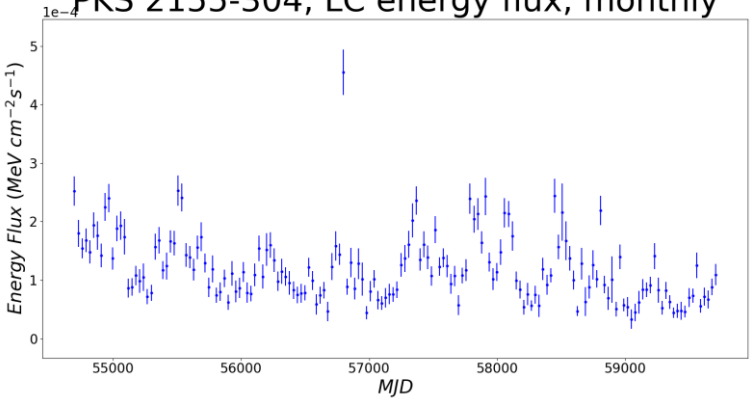

PKS 0405-385, WWZ & LSP, energy flux, monthly

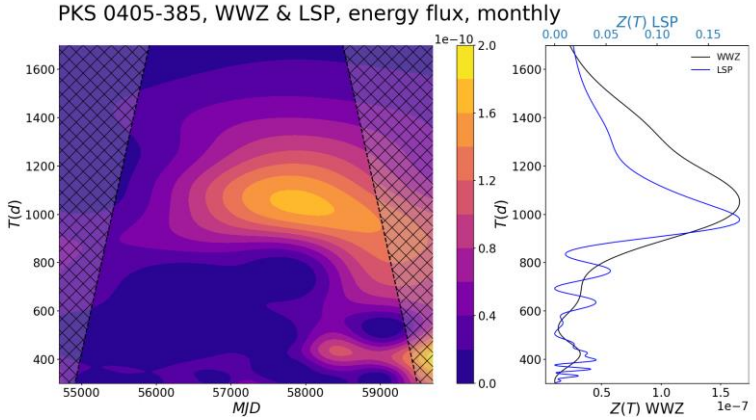

OJ 014, WWZ & LSP, photon flux, monthly

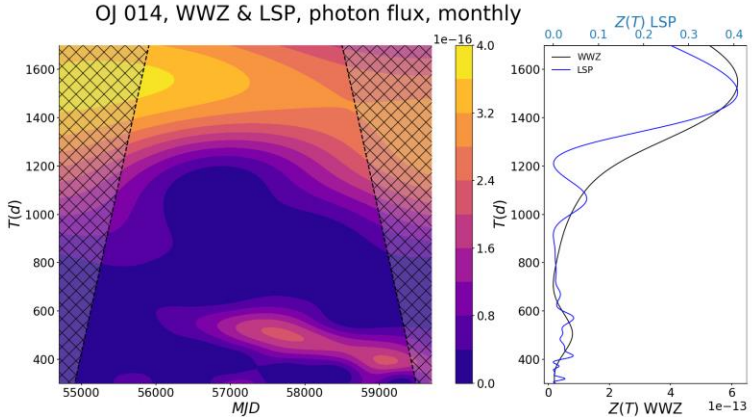

PKS 2155-304, WWZ & LSP, energy flux, monthly